AS-TEXONO/99-02
September 30, 1999

Prospects of Scintillating Crystal Detector in Low-Energy Low-Background Experiments

H.T. Wong [α, 1], J. Li [β], C.Y. Chang [γ], C.C. Chang [γ], C.P. Chen [α], W.P. Lai [α], H.B. Li [δ], Y. Liu [β], J.G. Lu [β], Z.P. Mao [β], S.C. Wang [α]

[α] Institute of Physics, Academia Sinica, Taipei, Taiwan.
[β] Institute of High Energy Physics, Beijing, China.
[γ] Department of Physics, University of Maryland, Maryland, U.S.A.
[δ] Department of Physics, National Taiwan University, Taipei, Taiwan.

Abstract

Scintillating crystal detector offers potential advantages in low-energy (keV-MeV range) low-background experiments for particle physics and astrophysics. The merits are discussed using CsI(Tl) crystal as illustrations. The various physics topics which can be pursued with this detector technology are summarized. A conceptual design for a generic detector is presented.

PACS Codes: 14.60.Pq; 29.40.Mc
Keywords: Neutrinos; Scintillation detector

(submitted to Astroparticle Physics)

[1] Corresponding Author. E-mail: htwong@phys.sinica.edu.tw

1 Introduction

Scintillating crystal detectors [1] have been widely used as electromagnetic calorimeters in high energy physics [2], as well as in medical and security imaging and in the oil-extraction industry. They have also been adopted for non-accelerator experiments, notably NaI(Tl) detectors are already used in Dark Matter searches [3], producing some of the most sensitive results.

Several characteristic properties make crystal scintillator an attractive detector option for low-energy (keV to MeV range) low-background experiments. Subsequent sections of this article will bring out the potential advantages of this approach and some of the physics topics well-suited to be investigated by this detector technology. The characteristic performance of the CsI(Tl) crystal are used as illustrations. A generic design to exploit these merits in a realistic experiment is discussed in Section 4.

2 Motivations and Merits

2.1 Nuclear Physics

The physics at the keV to MeV range can depend critically on the choice of isotopes as the interaction targets. The nuclear structure determines the interaction cross-sections, detection threshold, as well as experimental signatures like spatial or temporal correlations.

The deployment of target with large mass for low energy experiments usually requires that the target is an active detector. There are only a few detector technologies which accommodates a wide range of possible nuclei. The choice is even more limited when the potentials and possibilities to scale-up to a massive (tons or more) detector have to be taken into account. The two most prominent candidate techniques are loaded liquid scintillator and crystal scintillator.

2.2 Existing Experience and Potential Spin-Offs

The large target-mass requirement is always a challenge to low count rate experiments. From the big electro-magnetic calorimeters in high energy physics, there are much experience in producing and operating 50-ton-range crystal calorimeters. The technology is proven to be stable and robust at the harsh accelerator environment. Indeed, the present broad applications and affordable price range for crystals like CsI(Tl) and BGO are driven mostly by the demand and development from high energy physics experiments. Therefore, it is possible that construction of a big scintillating crystal detector for low-energy experiments will also lead to the maturity of a new technology with potential spin-offs in other areas.

2.3 Intrinsic Properties

Some of the properties of crystal scintillators make them favorable candidates to be adopted for studying low-energy low-background experiments. While different crystals do have different characteristic performance parameters, the merits of this detector approach are discussed below using CsI(Tl) as an illustration.

The characteristic properties of CsI(Tl) [4], together with a few other common crystals as well as liquid and plastic scintillators, are summarized and compared in Table 1. The selection of CsI(Tl) is due to the fact that it is a commonly used and relatively inexpensive crystal scintillator produced in large quantities and with many examples of successful operation as 50-ton-range electro-magnetic calorimeters, as in all the B-factory detectors currently under operation. Unlike NaI(Tl), it is only slightly hygroscopic and can operate stably for a long time without the need of a hermetic seal. This minimizes the use of passive materials at the target volume which, as explained below, is crucial to allow the merits of this detector technique for low-energy low-background experiments to be fully exploited.

2.3.1 Solid and Compact Detector

Crystal scintillators usually have high density and are made up of high-Z isotopes. Therefore, a massive (tens of tons) detector can still be very compact (scale of several m^3), such that external shielding configurations can be made more efficient and cost effective. The compact dimension also favors applications where artificial neutrino sources are used thereby allowing efficient exposure of the target materials to the source.

A solid detector can also prevent radioactive radon gas from diffusing into the inner fiducial volume from the external surfaces. This is a major concern for target based on gaseous or liquid detectors.

2.3.2 Efficient Active Veto

The attenuation effects of CsI(Tl) to γ-rays of different energy, together with those of water and liquid scintillator (a generic CH_2 compound with density 0.9 gcm^{-3}) [5], are depicted in Figure 1. In the region between 500 keV to around 3 MeV, Compton scattering (which varies as the atomic number Z) is the main process, and therefore the attenuation effects of CsI(Tl) are only enhanced by the density ratio, relative to H_2O and CH_2. Above several MeV, pair production (varying as Z^2) takes over making the high-Z CsI(Tl) more efficient. This is the reason of choosing this crystal as electromagnetic calorimeters. In the low energy region below 500 keV, photo-electric effects (varying as Z^5) dominates overwhelmingly. For instance, the attenuation lengths for a 100 keV γ-ray are 0.12 cm and 6.7 cm, respectively, for CsI(Tl) and CH_2. That is, 10 cm of CsI(Tl) has the same attenuating power as 5.6 m of liquid scintillator at this low energy. Most crystal scintillators, having high-Z isotopes, share this merit.

2.3.3 Focus only on Internal Background

Given the large attenuating effects on low energy photons, crystal detectors can provide a unique advantage to the background suppression in low energy experiments - that practically *all γ background originates internally.* For non-hygroscopic crystals like CsI(Tl) or BGO where a hermetic seal system is not needed for their operation, *"internal"* would include only two materials: the crystal itself and the surface wrapping or coating materials. Teflon wrapping sheets are most commonly used, while there is an interesting new development with sol-gel coating which can be as thin as a few microns [6].

Teflon is known to have very high radio-purity (typically better than the ppb level for the ^{238}U and ^{232}Th series) [7]. As a result, the experimental challenge and hurdle becomes much more focussed - the control and understanding of the internal purity of the crystal itself. The internal background can be due to contaminations of naturally occurring isotopes (^{238}U and ^{232}Th series, ^{40}K), long-lived fission products and cosmic ray-induced unstable nuclei.

The effects of external γ background, like those from the readout device, electronics components, construction materials, radon diffusion, are thus minimized. Background can also originate externally from cosmic-ray induced neutrons which have little attenuation with high-Z nuclei. Their effects, however, can be minimized by a cosmic veto and by operating the experiment underground.

Hygroscopic crystals like NaI(Tl) are housed in containers as hermetic seal. The containers, usually made of oxygen-free copper for low background application, can be made to have high radio-purity. However, it is still an inactive material with high cross-sections for photons. Consequently, it is possible that high energy photons (which has long attenuation length in the crystal) can penetrate into the fiducial volume, undergo Compton scatterings at the container, and deposit low energy at the crystal detector itself. Therefore, the adoption of non-hygroscopic crystals is essential to exploit the full power of this feature of eliminating all external gamma background.

The background count rate will be stable and not affected by external parameters if the dominant contributions are from internal contaminations. Therefore, this detector technique can provide additional desirable feature in applications requiring delicate comparison and subtraction of data taken at different periods (such as reaction ON/OFF, annual modulation, Day/Night effects).

2.3.4 Good Energy Resolution and Modularity

Light yield of typical crystal scintillators are comparable to those of liquid and plastic scintillators. However, the modular size are smaller while the refractive index higher, leading to more efficient light transmission and collection. The high gamma attenuation also allows full γ-energy deposition. Consequently, crystal scintillators have typically better energy resolution and lower detection threshold, both of which are necessary for low-energy measurements. The high γ-rays capture efficiency, together with the good resolution to measure them as energy-peaks, can provide important diagnostic tools for understanding the physical processes and background of the system. For instance, by measuring the γ-peaks due to ^{40}K, ^{60}Co and ^{137}Cs, their associated β-background can be accurately accounted for and subtracted off.

The good modularity also enhances background suppression, since the interesting signals for most applications are single-site events. Most background from internal radioactivity come as β+γ's in coincidence (like decays of ^{214}Bi and ^{208}Tl from the ^{238}U and ^{232}Th series, respectively) and hence will produce multiple hits with high probability. Similarly neutron capture events by the target isotopes manifest as (n,γ) interactions, giving rise to a γ-burst of multiple hits with known total energy. The neutron capture rate can therefore be measured, so that the background due to subsequent decays of the unstable daughter nuclei can be subtracted off.

2.3.5 Possibility of Pulse Shape Discrimination

Crystals like CsI(Tl) and NaI(Tl) have superb pulse shape discrimination (PSD) properties [8] to differentiate γ/e events from those due to heavily ionizing particles like α's, which have faster fall time. Figure 2 depicts typical PSD between α/γ in CsI(Tl) with the "Partial Charge Vs Total Charge" method [9], demonstrating excellent separation. The PSD capabilities provide powerful handle to tag and study those background channels involving alpha-emission, such as those from the ^{238}U and ^{232}Th decay chains.

2.3.6 High Sensitivity to U/Th Cascades

Unlike in liquid scintillators, α's are only slightly quenched in their light output in crystals like CsI(Tl) and NaI(Tl). The exact quenching ratio depends on the Tl concentration and the measurement parameters like shaping time: for full integration of the signals, the quenching is about 50% [4]. Therefore, some of the α's emitted from the uranium and thorium series are above 3 MeV. This is beyond the end-point for natural radioactivity (2.61 MeV) and hence the peak signatures are easy to detect among the flat background. In comparison, the electron-equivalence light yield for several MeV α's in liquid scintillators is typically less than 10% of their kinetic energy, making the signals well below the natural end-point and therefore more difficult to detect.

A crystal contaminated by uranium or thorium would therefore give rise to multiple peaks above 3 MeV, as reported in Ref. [10] in the case for CsI(Tl). Shown in Figure 3 is the background spectrum from a 5-kg CsI(Tl) crystal put in 5 cm of lead shielding with cosmic veto in a typical sea-level laboratory. The absence of multiple peaks above 3 MeV suggest a ^{238}U and ^{232}Th concentration of less than the 10^{-12} g/g level, assuming the decay chains are in equilibrium. All the peaks and structures in the spectrum can be explained by ambient radioactivity or by (n,γ) interactions at the crystal and shielding materials. This simple yet effective measurement for crystal scintillator can be compared to the complicated schemes requiring elaborate underground facilities for liquid scintillator [11]. A typical level achieve-able by the photon-counting method with a low-background germanium is only 10^{-9} g/g [7].

The sensitivities can be pushed further by doing the measurement underground (the flat background above 3 MeV are due to cosmic-ray induced neutrons which undergo (n,γ) when captured by the crystal or the shielding materials), and by exploiting the PSD characteristics of the crystal. In addition, by careful studies of the timing and energy correlations among the α's, one can obtain precise information on the radioactive contaminants in the cases where the ^{238}U and ^{232}Th decay series are not in equilibrium, so that the associated β/γ background can be accounted for accurately. For instance, some Dark Matter experiments with NaI(Tl) [3] reported trace contaminations (range of $10^{-18} - 10^{-19}$ g/g) of ^{210}Pb in the detector, based on peaks from γ's of 46.5 keV and from α's of 5.4 MeV. Accordingly, β-decays from ^{210}Bi can be subtracted off from the signal.

3 Potential Applications

Several areas of low energy particle physics where the crystal scintillator technique may be applicable are surveyed in this section.

3.1 Neutrino-Electron Scattering at Low Energy

Scatterings of the ($\nu_{\rm e}$ e) and ($\bar{\nu_{\rm e}}$ e) give information on the electro-weak parameters ($\rm g_V$, $\rm g_A$, and $\sin^2\theta_{\rm W}$), and are sensitive to small neutrino magnetic moments (μ_ν) [12]. They are two of the most realistic systems where the interference effects between Z and W exchanges can be studied [13].

The goal of future experiments will be to push the detection threshold as low as possible to enhance the sensitivities in the magnetic moment search. Using reactor neutrinos as source, an experiment based on a gaseous time projection chamber with CF_4 [14] is now operational. Another experiment using CsI(Tl) is being built [15], with the goal of achieving a threshold of 100 keV. Project with NaI(Tl) detector at an underground site and using an artificial neutrino source has also been discussed [16].

3.2 Neutral Current Excitation on Nuclei

Neutral current excitation (NCEX) on nuclei by neutrinos has been observed only in the case of ^{12}C [17] with 30 MeV neutrinos. Excitations with lower energies using reactor neutrinos have been studied theoretically [18] but not observed.

Crystal scintillators, having good γ resolution and capture efficiency, are suitable to study these processes where the experimental signatures are peaks in the energy spectra with characteristic energies. Realistic experiments can be based on using the crystal isotopes as active targets, like ^{133}Cs and ^{127}I in CsI(Tl) or ^{6}Li, ^{7}Li and ^{127}I in LiI(Eu). The ^{7}Li case, with a γ-energy of 480 keV, has particularly large cross-sections. Alternatively, a compact passive boron-rich target like B_4C can be inserted into an array of CsI(Tl) detector modules [15]. There are theoretical work [19] suggesting that the NCEX cross-sections on ^{10}B and ^{11}B are sensitive to the axial isoscalar component of NC interactions and the strange quark content of the nucleon.

3.3 Dark Matter searches

Direct searches of Weakly Interacting Massive Particles (WIMP) are based on looking for the low-energy (few keV) nuclear recoil signatures when they interact with the nuclei. Crystal scintillators may offer an appropriate detector technique for these studies from their PSD capabilities, as well as being a matured technology where a large target mass is possible. The cross-sections depend on specific isotopes [20], based on their nuclear matrix elements and spin states.

The scale of 100 kg of NaI(Tl) crystal detectors [3] are already used in WIMP searches and produce some of the most sensitive results. Other cases like CaF_2 [21] are also pursued.

For crystal detectors where a three-dimensional fiducial volume with minimal passive materials can be defined, there is no background due to external γ's at this low energy. Internal β background is suppressed by the spectral distribution at this very low energy range. For instance, less than $3{\times}10^{-4}$ of the β-decays in ^{40}K (end-point 1.3 MeV), give rise to events below 10 keV. Therefore, nuclear recoils due to neutrons will be the major background channels

3.4 Low Energy Solar Neutrinos

The goal of future solar neutrino experiments will be to measure the low energy (pp and ^7Be) solar neutrino spectrum. Charged- (CC) and Neutral-current (NC) on nuclei are attractive detection channels besides neutrino-electron scattering. The CC mode can provide a direct measurement of the ν_e-spectrum from the Sun without the convolutions necessary for the ν-e channels, while the NC mode can provide a solar model independent cross-check. Crystal scintillators are possible means to realize detectors based on the CC and NC interactions.

Previously, crystals with indium has been investigated [22] for a $\nu_\odot$-detector with ^{115}In as target which can provide a distinct temporally and spatially correlated triple coincidence signature. Recently, the crystals LiI(Eu) [23] and GSO ($Gd_2SiO_5(Ce)$) [24]

are being considered. The attractive features are that LiI(Eu) have large ν_eN-CC cross-sections for both ^{7}Li and ^{127}I, and ν_eN-NC (E_γ=480 keV) for ^{7}Li, while ^{160}Gd in GSO can provide another time-delay signature for background suppression and for tagging the flavor-specific ν_eN-CC reactions.

4 Generic Detector Design

To fully exploit the advantageous features discussed in Section 2, the design of a scintillating crystal detector for low-energy low-background experiments should enable the definition of a fiducial volume with a surrounding active 4π-veto.

Displayed in Figure 4 is a generic conceptual design where such a detector can be realized. The detector design is based on an experiment being constructed [15] which, in its first phase, will study low energy neutrino-electron scattering from reactor neutrinos using CsI(Tl) as target. The listed dimensions are for this particular experiment. The dimensions for other applications will naturally depend on the optimization based on the specific detector performance and requirements.

As shown in Figure 4, one CsI(Tl) crystal unit consists of a hexagonal-shaped cross-section with 2 cm side and a length 20 cm, giving a mass of 0.94 kg. Two such units are glued optically at one end to form a module where the light output from both ends are read out by photo-detectors. Photo-multipliers (PMTs) with potassium-free glass window will be used for the experiment though solid-state photo-detectors like photo-diodes or avalanche photo-diodes are also possibilities for other applications. The modular design enables the detector to be constructed in stages. Figure 4 shows a design with a 17$\times$15 matrix giving a total mass of 480 kg.

The energy deposited can be derived from the sum of the two PMT output ($Q_{tot} = Q_1 + Q_2$) after their gains are normalized, while the longitudinal position can be obtained from their difference in the form of $R = (Q_1 - Q_2)/(Q_1 + Q_2)$. The variation of Q_1, Q_2 and Q_{tot} along the crystal length are displayed in Figure 5. The error bars denote the width of the photo-peaks of a ^{137}Cs source. The discontinuity in the middle is due to the optical mismatch between the interface glue (n=1.5) and the crystal (n=1.8). It can be seen that Q_{tot} is independent of the position, and the resolution at 660 keV is about 10%. The detection threshold (where signals are measured at both PMTs) is <20 keV.

The variation of R along the crystal length is depicted in Figure 6. The ratio of the RMS errors in R relative to the slope gives the longitudinal position resolution. Its variation as a function of energy, obtained by analyzing the different energy-bins of the ^{137}Cs spectra, is displayed in Figure 7, showing a resolution of 2 cm and 3.5 cm at 660 keV and 200 keV, respectively. Accordingly, a three-dimension fiducial volume can be defined, where the definitions can be optimized for different energy ranges. CsI(Tl) is only slightly hygroscopic, so that the fiducial volume consists of only the crystal itself and the teflon wrapping sheets, typically in a mass ratio of 1000:1.

The various potential experiments based on scintillating crystal detectors can essentially adopt a similar design. Much flexibility is available for optimization. Different modules can be made of different crystals. Different crystals can be glued together, in which case the event location among the various crystals can be deduced from the different pulse shape. Passive target can be inserted to replace a crystal module.

5 Outlook

Large water Cerenkov and liquid scintillator detectors have been successfully used in neutrino and astro-particle physics experiments. New detector technology must be explored to open new windows of opportunities. Crystal scintillators may be well-suited to be adopted for low background experiments at the keV-MeV range. Pioneering efforts have already been made with NaI(Tl) crystals for Dark Matter searches, while another experiment with CsI(Tl) is being constructed to study low energy neutrino interactions. The present O(100 kg) target mass range can be scaled up to tens of tons, based on the successful experience of calorimeters in high energy physics experiments.

A generic detector design is considered in this article, demonstrating that defining a three-dimensional fiducial volume with minimal passive materials is possible. The large γ-attenuation at low energy can lead to a large suppression of background due to ambient radioactivity by the active veto layers. Consequently, the key experimental challenge becomes one focussed on the understanding, control and suppression of the radioactive contaminations in the crystals. The high γ-detection efficiency, good energy and spatial resolutions, low detection threshold, PSD capabilities and clean alpha signatures provide powerful diagnostic tools towards these ends.

There are still much room for research and development towards the realization of big experiments. Potential spin-offs in other areas are possible in the course of these efforts.

This work was supported by contracts NSC 87-2112-M-001-034 and NSC 88-2112-M-001-007 from the National Science Council, Taiwan.

References

[1] For a recent review on the crystal scintillator detector, see, for example,
M. Ishii and M. Kobayashi, Prog. Crystal Growth and Charact., **23**, 245 (1991), and references therein.

[2] For a recent review on the applications of crystal scintillator in particle physics, see, for example
G. Gratta, H. Newman, and R.Y. Zhu, Ann. Rev. Nucl. Part. Sci. **44**, 453 (1994).

[3] K. Fushimi et al., Phys. Rev. **C 47**, R425 (1993);
M.L. Sarsa et al., Nucl. Phys. **B 35**, 154 (1994);
N.J.C. Spooner et al., Phys. Lett. **B 321**, 156 (1994);
R. Bernabei et al., Phys. Lett. **B 389**, 757 (1996);
R. Bernabei et al., Phys. Lett. **B 450**, 448 (1999);
G. Gerbier et al., Astropart. Phys. **11**, 287 (1999).

[4] H. Grassman, E. Lorentz, and H.G. Moser, Nucl. Instrum. Methods **228**, 323 (1985);
P. Schotanus, R. Kamermans, and P. Dorenbos, IEEE Trans. Nucl. Sci. **37**, 177 (1990).

[5] E. Storm and H.I. Israel, Nucl. Data. Tables **A7**, 565 (1970).

[6] R. Chipaux et al., DAPNIA-SED-98-01, to be published in IEEE Trans Nucl. Sci. (1999).

[7] P. Jagam and J.J. Simpson, Nucl. Instrum. Methods **A 324**, 389 (1993).

[8] J. Alarja et al., Nucl. Instrum. Methods **A 242**, 352 (1986);
P. Kreutz et al., Nucl. Instrum. Methods **A 260**, 120 (1987).

[9] C.L. Morris et. al., Nucl. Instrum. Methods **137**, 397 (1976);
M.S. Zucker and N. Tsoupas, Nucl. Instrum. Methods **A299**, 281 (1990).

[10] U. Kilgus, R. Kotthaus, and E. Lange, Nucl. Instrum. Methods **A 297**, 425, (1990);
R. Kotthaus, Nucl. Instrum. Methods **A 329**, 433 (1993).

[11] G. Alimonti et al., Nucl. Instrum. Methods **A 406**, 411 (1998).

[12] P.Vogel and J.Engel, Phys. Rev. **D 39**, 3378 (1989).

[13] B. Kayser et al., Phys. Rev. **D 20**, 87 (1979).

[14] C. Amsler et al., Nucl. Instrum. Methods **A 396**, 115 (1997).

[15] H..T. Wong and J. Li, Nucl. Phys. **B** (Proc. Suppl.) **77**, 177 (1999)

[16] I.R. Barabanov et al., Astropart. Phys. **5**, 159 (1996).

[17] B. Armbruster et al., Phys. Lett. **B 423**, 15 (1998).

[18] H.C. Lee, Nucl. Phys. **A 294**, 473 (1978) ;
T.W. Donnelly and R.D. Reccei, Phys. Rep. **50**, 1 (1979).

[19] T. Suzuki, Y. Kohyama, and K. Yazaki, Phys. Lett. **B 252**, 323 (1990);
J. Bernabéu et al., Nucl. Phys. **B 378**, 131 (1992);
K. Kubodera and S. Nozawa, Int. J. Mod. Phys. **E 3**, 101 (1994).

[20] J. Ellis, R.A. Flores and J.D. Lewin, Phys. Lett. **B 212** 375 (1988);
J. Ellis and R.A. Flores, Phys. Lett. **B 263** 259 (1991).

[21] C. Bacci et al., Astropart. Phys. **2**, 117 (1994).

[22] R.S. Raghavan, Phys. Rev. Lett. **37**, 259 (1976);
M. Avenier et al., Nucl. Phys. **B** (Proc. Suppl.) **28A**, 496 (1992).

[23] C.C. Chang, C.Y. Chang, and G. Collins, Nucl. Phys. (Proc. Suppl.) **B 35**, 464 (1994).

[24] R.S. Raghavan, Phys. Rev. Lett. **78**, 3618 (1997).

Properties	CsI(Tl)	NaI(Tl)	BGO	Liquid	Plastic
Density (gcm^{-3})	4.51	3.67	7.13	0.9	1.0
Relative Light Yield	0.45	1.00 †	0.15	0.4	0.35
Radiation Length (cm)	1.85	2.59	1.12	$\sim$45	$\sim$45
dE/dx for MIP ($MeVcm^{-1}$)	5.6	4.8	9.2	1.8	1.9
Emission Peak (nm)	565	410	480	425	425
Decay Time (ns)	1000	230	300	2	2
Refractive index	1.80	1.85	2.15	1.5	1.6
Hygroscopic	slightly	yes	no	no	no

† Typical light yield for NaI(Tl) is about 40000 photons per MeV.

Table 1: Characteristic properties of the common crystal scintillators and their comparison with typical liquid and plastic scintillators.

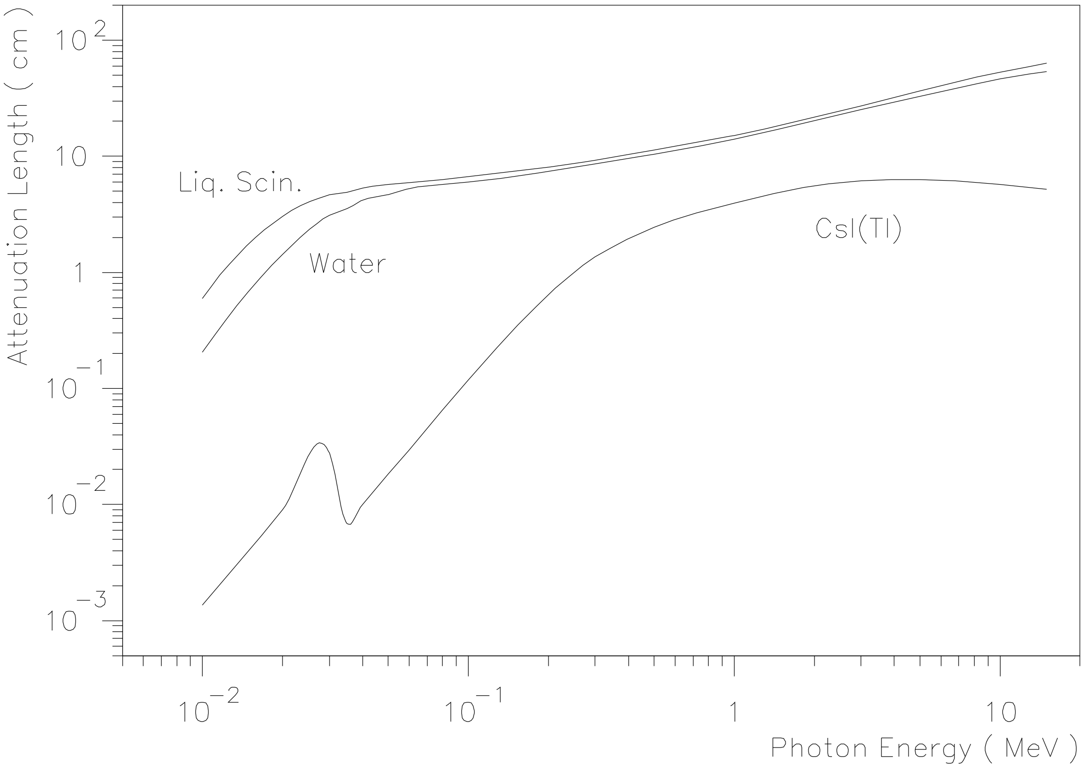

Figure 1: The attenuation length, as defined by the interactions that lead to a loss of energy in the media, for photons at different energies, for CsI(Tl), water, and liquid scintillator.

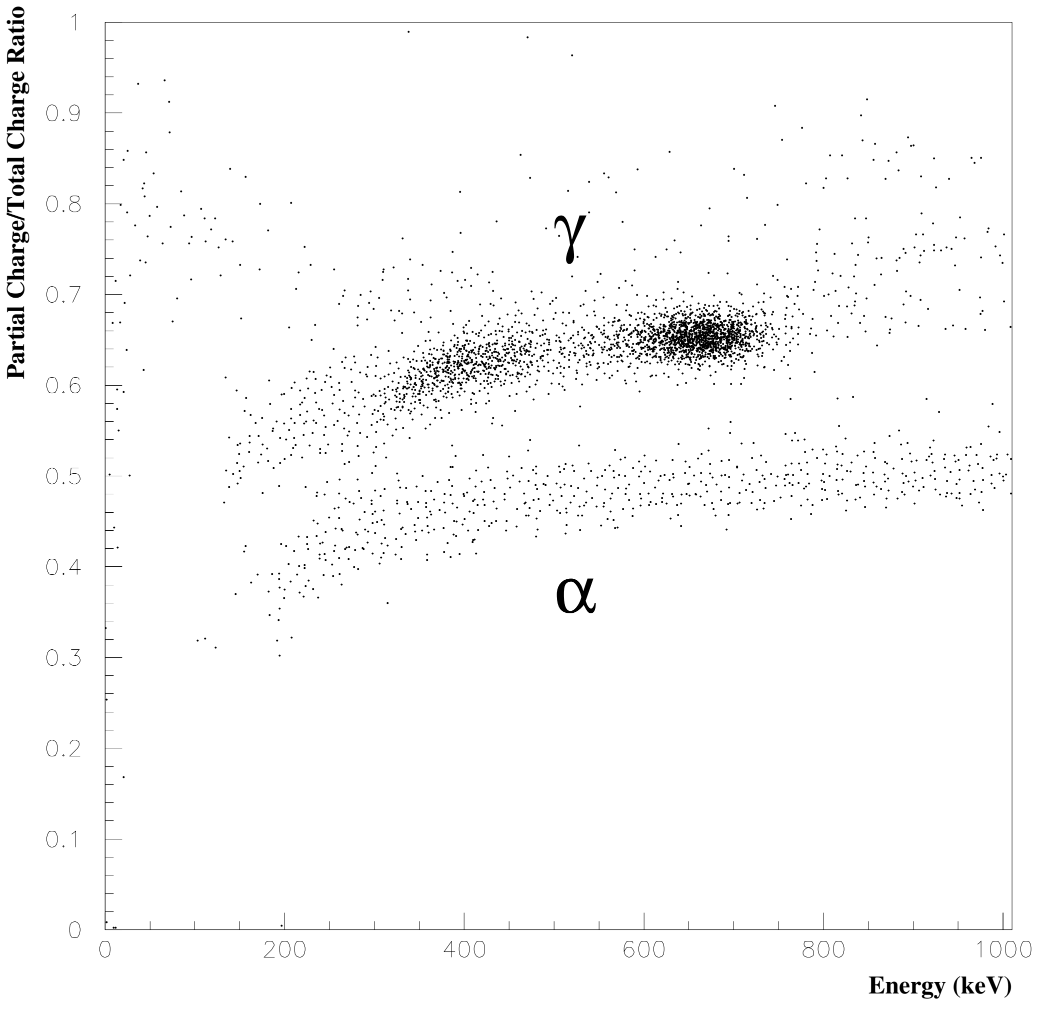

Figure 2: The partial charge/total charge ratio in a CsI(Tl) crystal as a function of energy, showing excellent pulse shape discrimination capabilities to differentiate events due to α's and γ's. The γ-events are due to a ^{137}Cs source, showing peaks at the full-energy and Compton edge regions. The α-events are from the low-energy tails of an ^{241}Am-Be source placed on the surface of the crystal.

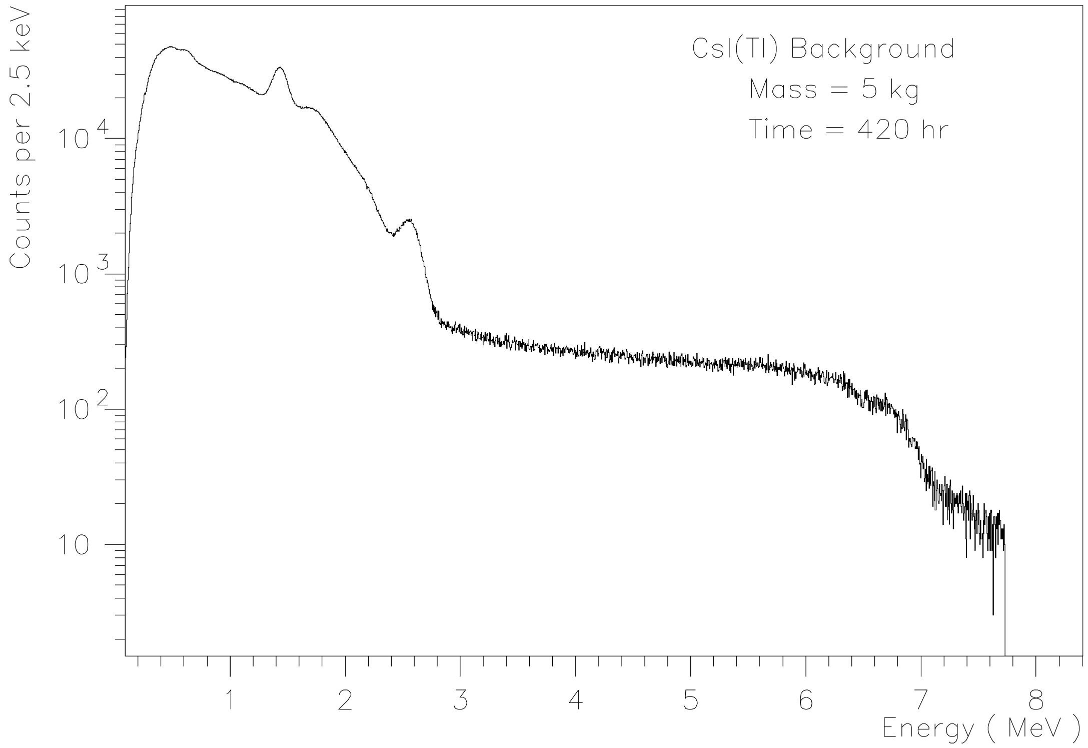

Figure 3: Measured background spectrum of a 5 kg CsI(Tl) under lead shieldings and cosmic-ray veto. The absence of peaks above 3 MeV provides sensitive limits to contaminations of ^{238}U and ^{232}Th decay chains in equilibrium.

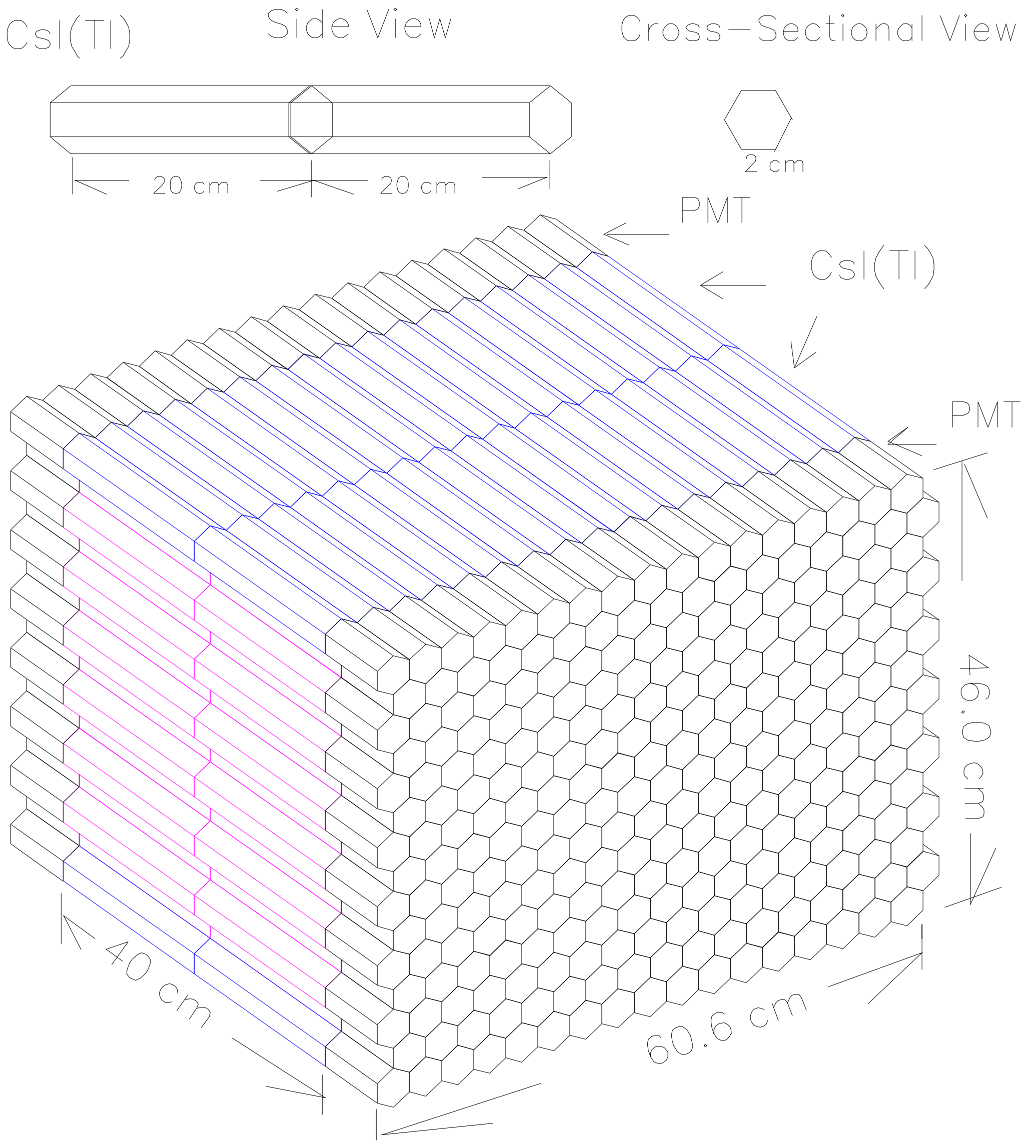

Figure 4: The schematic design of a generic scintillating crystal detector.

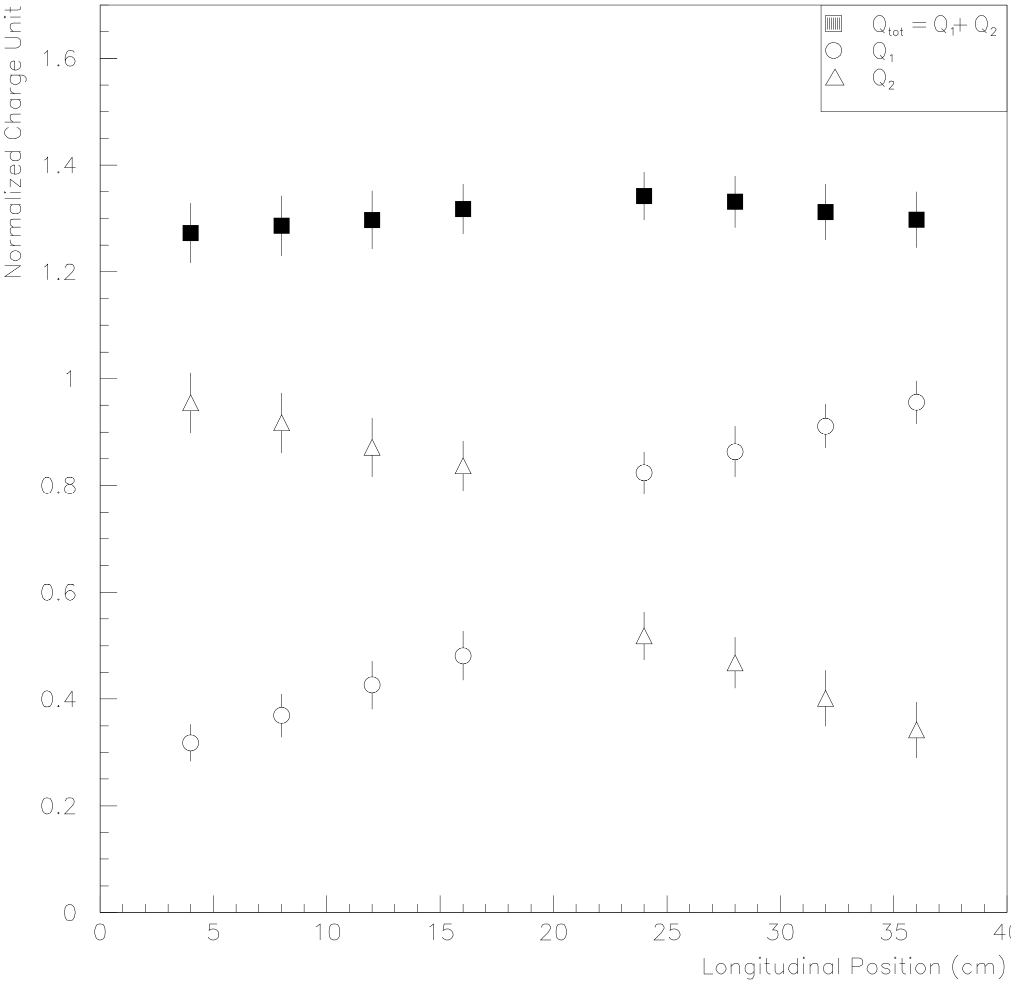

Figure 5: The measured variations of Q_1, Q_2 and $Q_{tot} = Q_1 + Q_2$ along the longitudinal position of the crystal module. The charge unit is normalized to unity for both Q_1 and Q_2 at their respective ends. The error bars denote the width of the photo-peaks due to a ^{137}Cs source.

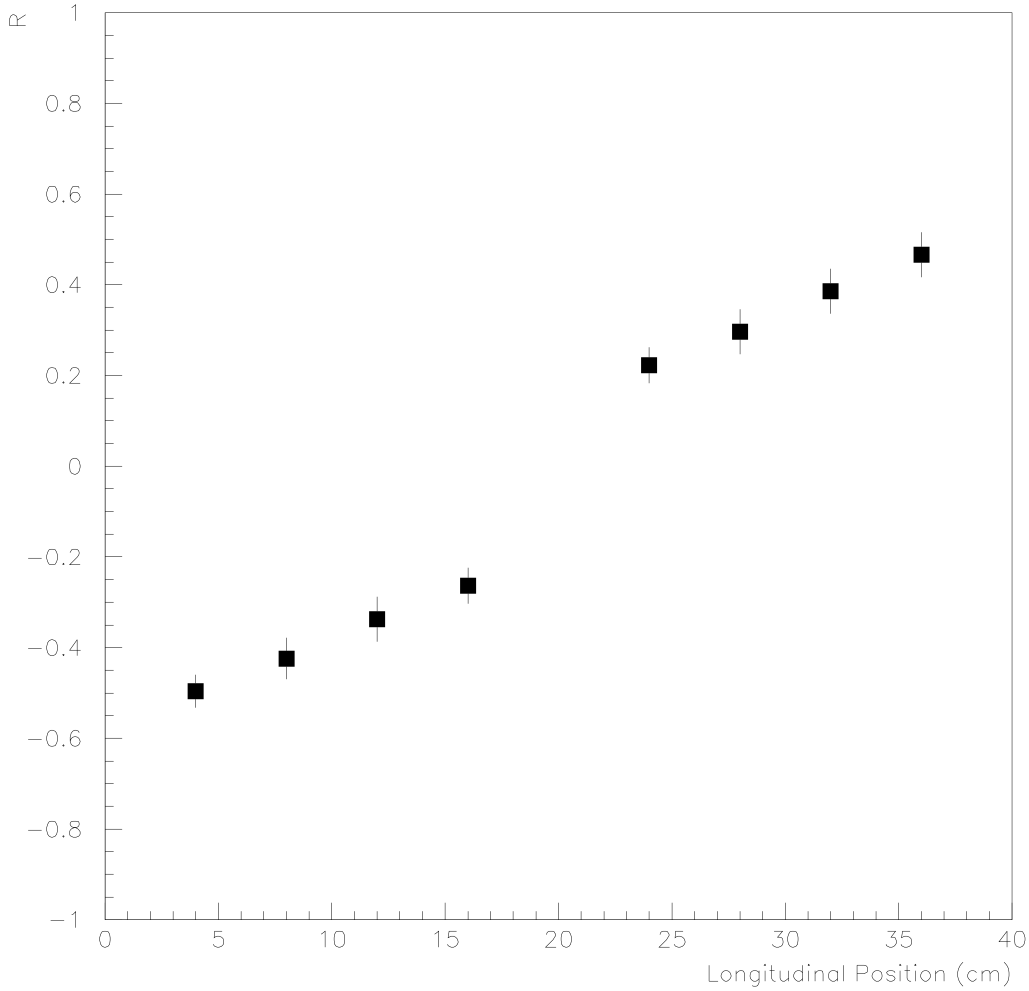

Figure 6: The variation of $R = (Q_1 - Q_2)/(Q_1 + Q_2)$ along the longitudinal position of the crystal module, showing the capability to provide a position measurement.

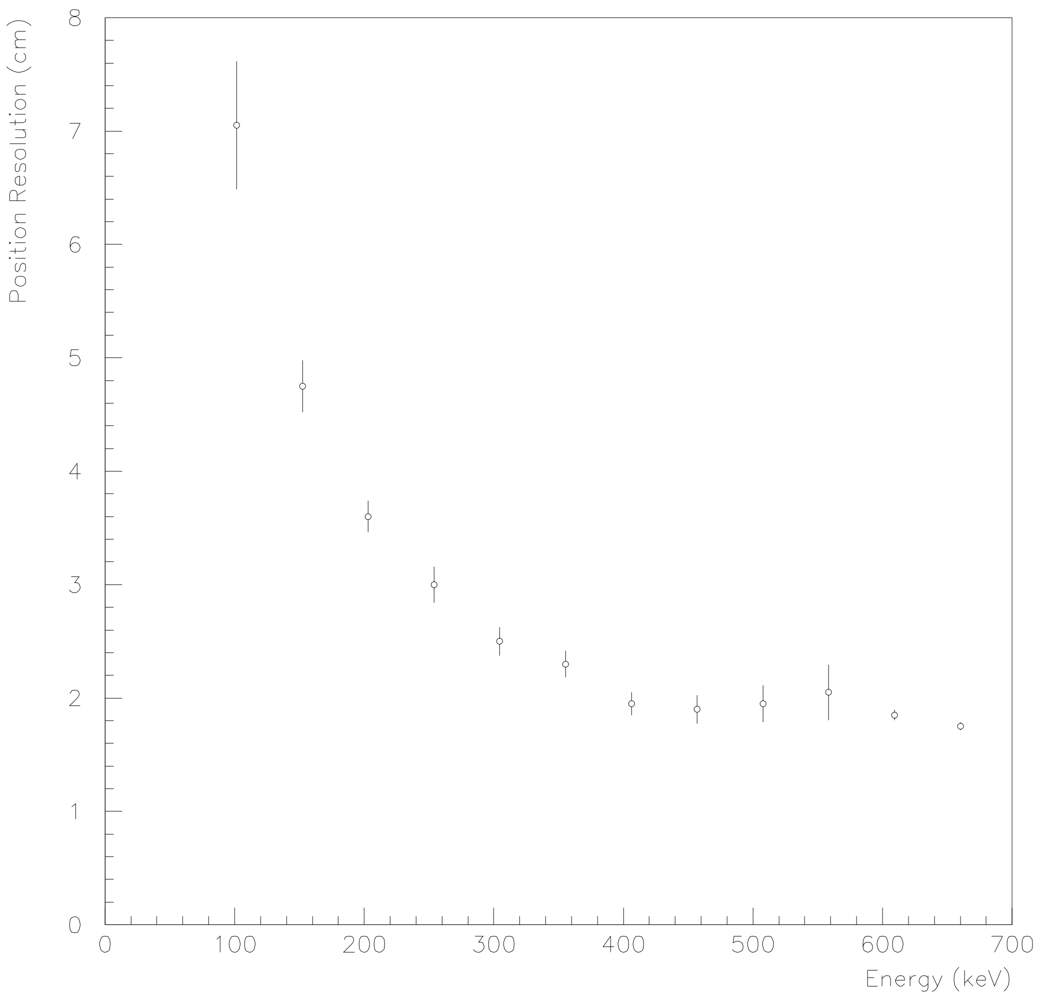

Figure 7: The variation of longitudinal position resolution as a function of gamma-energy, obtained by analyzing the different energy-bins in spectra due to a ^{137}Cs γ-source.